

# A New Model for Designing Multi-hole Multi-permeability Nonlinear LTCC inductors

Laili Wang, Zhiyuan Hu, Yajie Qiu, Hongliang Wang, Yan-Fei Liu

Department of Electrical and Computer Engineering  
Queen's University  
Kingston, ON, Canada  
lailiwang@gmail.com

**Abstract**—Nonlinear inductors have wide applications in DC/DC converters. The multi-hole multi-permeability nonlinear inductors have been proved to have gradually changing wide-range inductance curve while requiring no extra DC bias, which makes them suitable in various high efficiency DC/DC converters. This paper focuses on the design of such a multi-hole multi-permeability inductor. In the conventional design, complicated simulation needs to be executed when the coupling matrix among all the holes are taken into consideration. A dedicated model for calculating the inductance value is proposed in this paper to reduce the complexity. In the proposed model, the inductance simulation is simplified to calculating inductance of three basic units which are included in a nine-hole inductor. By simulating the nine-hole inductor, inductance of any rectangle shape multi-permeability nonlinear inductor with any number of evenly distributed holes on it can be calculated. Based on the proposed model, design guideline of the nonlinear inductor is also summarized. A sixteen-hole, two-permeability prototype is presented to demonstrate the design process according to the new model. The complete simulation and the test results are also provided to verify the model. The proposed model correlate with the simulation results very well.

## I. INTRODUCTION

The nonlinear inductors are widely used to optimize DC/DC converters for specific purposes. In the past twenty years, they attract extensive attentions from both academic research field and industrial field. The nonlinear inductor can be used in main circuit of buck converters [1], boost converters [2], phase-shift-full-bridge converters [3], forward converters [4], resonant converters [5]. In above literatures, the nonlinear inductors are used in the main circuit to realize soft switching. To further reduce the power loss, cost, and size, a nonlinear inductor together with a capacitor is employed to realize zero-voltage-switching (ZVS) in [6]. This method is further extended to be used in a multiple phase application [7]. Besides soft switching, the nonlinear inductors can also be used in resonant converters to realize constant frequency control [8-9] and to improve the dimming characteristics in lighting applications [10]. For the inductors in above literatures, the changing inductance curves are

realized by controlling the extra DC bias. But there are two disadvantages of these inductors, hindering their popularity in industry applications. First, they require DC biases, which cause extra loss and partly offset their advantages. Second, the inductance changes too fast with respect to the change of DC bias. Third, the nonlinear inductors are designed with commercial ferrite magnetic cores, which has different temperature expansion coefficient (TEC) with silicon, thus can't be integrated with silicon directly. A nonlinear inductor without extra DC bias is elaborated in [11] to eliminate the extra loss caused by DC bias. To achieve better characteristics than the conventional nonlinear inductors, multi-hole multi-permeability nonlinear inductors based on low temperature co-fired ceramic technology (LTCC) were proposed in [12]. The multi-hole multi-permeability nonlinear inductors have more gradually changing wide-range inductance value curves, which agrees very well with desired requirements of some power applications. Furthermore, the inductors are distributed air-gap and don't need extra DC biases, which make them suitable to improve the efficiency of converters. LTCC is a very high density multi-layer packaging technology in which very thin magnetic tapes, capacitor tapes, ceramic tapes are co-fired together to form an integrated substrate. Since ceramic tapes have nearly the same temperature expansion coefficient (TEC) with silicon, LTCC technology has high potential to be used to make highly integrated DC/DC converters as shown in Fig. 1.

The multi-hole multi-permeability nonlinear inductors are co-fired with ferrite tapes of different permeability. Fig. 2 shows the structure of a sixteen-hole square shape multi-hole multi-permeability inductor. The holes evenly distribute on the magnetic core with wires going up and down. By configuring the permeability values and thickness of the co-fired ferrite tapes, the desired inductance characteristics could be obtained for different applications. However, design of such an inductor requires complicated computer aided finite element analysis (FEA), which is a very time consuming process.

This paper proposes a new model to simplify the design of a multi-hole multi-permeability rectangular shape nonlinear LTCC inductor with evenly distributed holes on it.

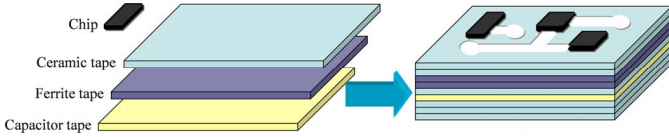


Fig. 1 Structure of an integrated DC/DC converter based on LTCC technology.

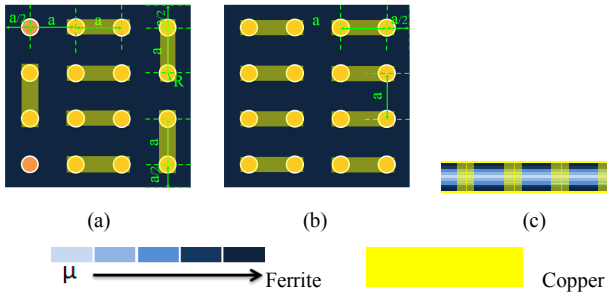


Fig. 2 A sixteen-hole multi-permeability LTCC nonlinear inductor. (a) Top. (b) Bottom. (c) Cross-section view.

## II. NEW MODEL OF THE MULTI-HOLE MULTI-PERMEABILITY NONLINEAR INDUCTORS

Modeling of nonlinear inductors has been investigated for long time, and there have been a lot of literatures discussing about the simplification of the inductance calculation models [13-17]. However, the models in these literatures are mainly based on the conventional commercial magnetic cores, and can't be applied to the new proposed multi-hole multi-permeability nonlinear inductors.

As shown in Fig. 2, several parameters require being determined in the design process of the multi-hole multi-permeability inductor. They are the permeability values, total permeability number, distance between adjacent holes, radius of the holes, coupling coefficients between holes for different permeability. To finish the design process by taking all the five parameters into account, complicated finite element analysis (FEA) simulations should be executed. However, the inductance calculation process based on FEA is very time-consuming, especially in iterated design process. This is mainly because there are coupling coefficients between each hole and all the other holes on the substrate, and all the couplings need to be fully taken into account during the simulation process. In the design process, the calculation process can be greatly simplified if the couplings between holes are completely neglected, but it will result in a big inaccuracy of the calculated inductance value. To simplify the design of a multi-hole nonlinear inductor while still maintaining the design accuracy, a new model is proposed in this paper which only considers the couplings between adjacent holes. Since the adjacent holes have much stronger coupling than those further away, the latter can be neglected. Thus the holes in the substrate can be classified into three types, the first type being the holes at four corners, defined as Unit 1; the second type being the holes along the sides except

for those at the corners, defined as Unit 2; the third type being the holes at the inner side of the substrate, defined as Unit 3. Fig. 3(a) shows a twenty-five-hole two-permeability nonlinear inductor. The point markers in the holes indicate the current flows from the bottom to the top while the cross markers in the holes indicate the current flows from the top to the bottom. It can be seen that, for each hole, the adjacent holes on the same row or the same column have the opposite current directions, whereas the adjacent holes on the oblique lines have the same current direction. Holes with opposite current directions have the negative coupling coefficients, and holes with the same current directions have positive coupling coefficients. Each Unit 1 hole has two negatively coupled holes and one positively coupled hole. Each Unit 2 hole has three negatively coupled holes in straight lines and two positively coupled holes in oblique lines. Each Unit 3 hole has four negatively coupled holes in straight lines and four positively coupled holes in oblique lines. In the new model, the total inductance calculation can be obtained by multiplying the number of each unit and the inductance of the unit which is contributed by the hole and its adjacent coupling holes. FEA simulation is still a highly efficient way to calculate the inductance of each unit accurately. A nine-hole square shape inductor is the smallest inductor which includes all the three units, therefore, the inductance of each unit and their coupling coefficients in any multi-hole nonlinear inductor can be simulated in a nine-hole square shape inductor featuring the same magnetic material characteristics, the same hole radius, and the same distance between the holes.

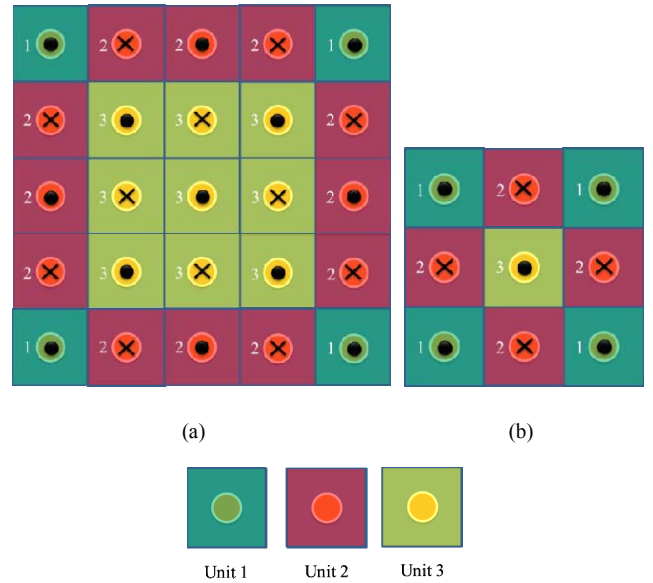


Fig. 3 A twenty-five-hole two-permeability LTCC nonlinear inductor and its nine-hole simulation block.

In this way, design of any multi-hole multi-permeability nonlinear inductor with holes evenly distributing on the rectangular substrate can be simplified to the inductance simulation of a nine-hole multi-permeability nonlinear inductor. Thus there are three steps in the new simplified model. Firstly, the multiple holes on the multi-permeability rectangular magnetic substrate are classified into three basic

units. Then the inductance contributed by each unit can be obtained by simulating a nine-hole nonlinear inductor as shown in Fig. 3(b). Finally, the total inductance is obtained by multiplying the inductance of each unit and their corresponding quantities.

To calculate the nonlinear inductance of each unit, incremental flux/current as shown in (1) should be used. The expressions for inductance calculation of Unit 1, Unit 2 and Unit 3 are shown in (2), (3), (4).

$$L = \frac{\Delta\Phi}{\Delta I} \quad (1)$$

In each permeability magnetic material  $p_i$ , the coupling coefficients are classified into four values. The first one is the coupling coefficient between Unit 1 and Unit 2  $k_{pi-12}$ ; the second one is the coupling coefficient between Unit 1 and Unit 3  $k_{pi-13}$ ; the third one is the coupling coefficient between Unit 2 and Unit 3  $k_{pi-23}$ ; the last one is coupling coefficient between two Unit 2 cells  $k_{pi-22}$ .

$$L_{pi-u1}(I) = \frac{\Delta\Phi_{pi}(1 + 2k_{pi-12} + k_{pi-13})}{\Delta I} \quad (2)$$

$$L_{pi-u2}(I) = \frac{\Delta\Phi_{pi}(1 + 2k_{pi-12} + 2k_{pi-22} + k_{pi-23})}{\Delta I} \quad (3)$$

$$L_{pi-u3}(I) = \frac{\Delta\Phi_{pi}(1 + 4k_{pi-13} + 4k_{pi-23})}{\Delta I} \quad (4)$$

In above three equations,  $\Delta I$  is the incremental current; and  $\Delta\Phi_{pi}$  is the incremental flux generated by incremental current flowing though each hole in magnetic material  $p_i$ .

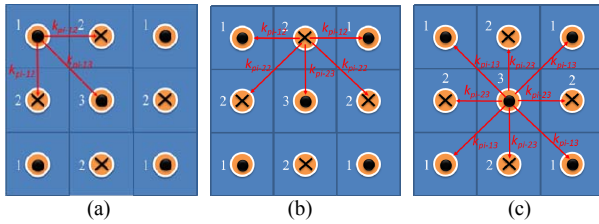


Fig. 4 Adjacent coupling holes of each unit in a nine-hole inductor.  
(a) Unit 1. (b) Unit 2. (c) Unit 3

Inductance contributed by each permeability magnetic material is expressed by (5). For a multi-hole multi-permeability inductor which contains  $m$  kinds of permeability, the total inductance can be calculated by adding up the inductances contributed by each magnetic material as shown in (6).

$$L_{pi}(I) = n_1 L_{pi-u1}(I) + n_2 L_{pi-u2}(I) + n_3 L_{pi-u3}(I) \quad (5)$$

$$L(I) = \sum_{i=1}^m h_i L_{pi} \quad (6)$$

Where  $h_i$  is the thickness of each permeability magnetic material.  $n_1, n_2, n_3$  are number of unit 1, unit 2, and unit 3, respectively.

DCR of the inductor can be calculated according to (7)

$$R_{DCR} = n \frac{\rho h_i}{\pi R^2} + (n-1) \frac{\rho a}{Rh_c} \quad (7)$$

Where  $n$  is the number of the total holes,  $\rho$  is the resistivity of copper,  $h_i$  is the thickness of magnetic core,  $h_c$  is the conductor thickness of the copper on the top and bottom.

To verify the accuracy of the new model, the twenty-five-hole two-permeability inductor is simulated to compare the results obtained through the model and the simulation. Fig. 4 shows the adjacent coupling holes of each unit. Twenty five holes distribute on the substrate evenly. The radius of the hole is 0.75mm; the distance between two holes is 4mm; and the distance between edges and their closest holes is 2mm. Two kinds of magnetic materials are selected. One has a relative permeability 50, and the other one has a relative permeability 200. As analyzed above, the first step is to classify the holes into three units. The second step is using equations (2), (3), (4) to calculate the inductances contributed by each unit, which can be obtained by simulating a nine-hole inductor that has the same magnetic materials, radius of holes, and distance between holes. The last step is to calculate the total inductance according to the (5). In the comparison, the thickness of  $\mu_r=50$  magnetic material is 2mm; the thickness of  $\mu_r=200$  magnetic material is 1mm. Fig. 5, Fig. 6, Fig. 7 show the comparison results of the simulation and modeling for  $\mu_r=50$  magnetic material,  $\mu_r=200$  magnetic material, and total inductance respectively when output current increases from 0A to 10A. The maximum inductance errors for  $\mu_r=50$  and  $\mu_r=200$  magnetic material are 4% and 3.2%, respectively. For the total inductance, the inductance error is 3.6%. It can be seen that the proposed model is very accurate to calculate the inductance value.

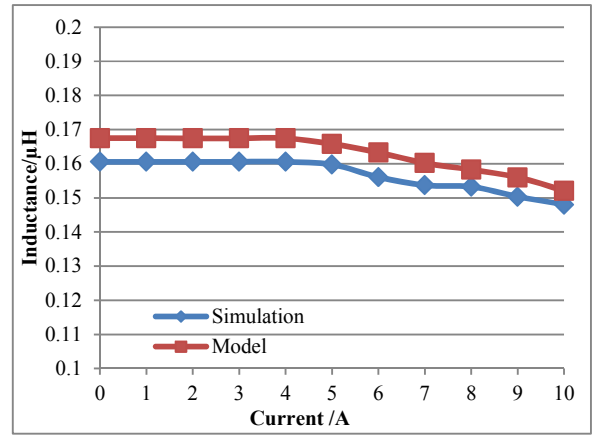


Fig. 5 Inductances based on the simulation and model for  $\mu_r=50$ .

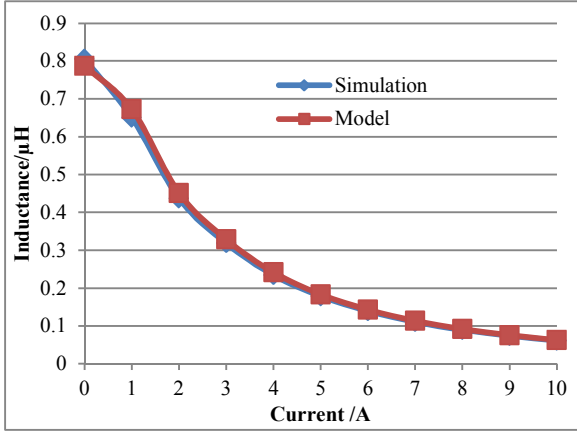


Fig. 6 Inductances based on the simulation and model for  $\mu_r=200$ .

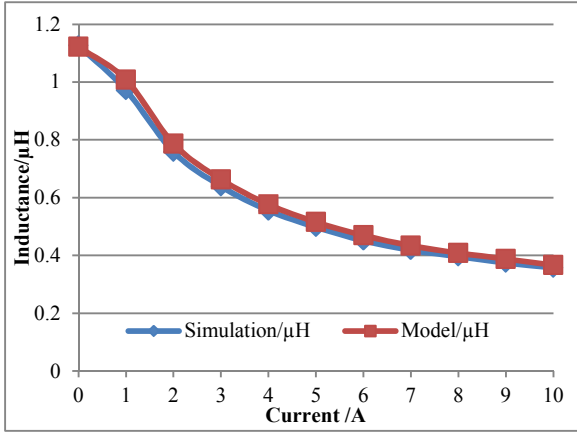


Fig. 7 Total inductances of the twenty-five-hole inductor based on the simulation and model.

### III. DESIGN OF A MULTI-HOLE MULTI-PERMEABILITY INDUCTOR

In this section, design of a multi-hole multi-permeability inductor will be demonstrated by designing a 3mm thick, sixteen-hole two-permeability inductor ( $0.8\mu\text{H}@0\text{A}$ ,  $0.3\mu\text{H}@10\text{A}$ ). For a general design, the holes distance  $a$  and hole radius  $R$  should also be seen as variables for iterated calculation of design process. The design guideline can be summarized as follows.

- Determine the number of different permeability materials in the multi-permeability inductor.
- Classify the holes into three basic units. Simulate the inductance values of each unit in a nine-hole inductor for different holes distance  $a$ , hole radius  $R$ . Repeat the simulation for each permeability material.
- Calculate the inductances of a sixteen-hole inductor versus output current for each configurations

- according to (5). Repeat the calculation for each permeability material.
- d. Calculate the thickness values of each permeability magnetic material in the inductor for each configuration according to (6). There might be more than one solution for the equations.
- e. Calculate DCR of the inductor for different configurations according to (7).
- f. Determine the holes distance  $a$  and hole radius  $R$  by compromising the inductance and DCR.

In the new design, two kinds of LTCC ferrite tapes will be used. Their relative permeabilities are 50 and 200. As described in Section II, the calculation of a multi-hole inductor can be simplified to a nine-hole inductor; the design of a multi-hole inductor can also be simplified to iterated simulation of a nine-hole inductor. With radius  $R$  and holes distance  $a$  as parameters, two nine-hole inductors composed of  $\mu_r=50$  ferrite tapes, and  $\mu_r=200$  ferrite tapes are simulated.

Several configurations of radius and holes distance are selected for simulation in order to calculate their inductances versus output current. Fig. 8 and Fig. 9 show the inductances versus output current for  $\mu_r=50$  ferrite tapes and  $\mu_r=200$  ferrite tapes with different configurations.

DCR of the inductor for different configurations are also calculated. Fig. 10 shows the results. With the increase of side length, DCR of the inductor gradually increases, but at certain side length, the DCR has a decreasing trend with the increase of the radius.

By compromising the inductance values and DCR,  $a=4.5\text{mm}$ ,  $R=0.75\text{mm}$  are selected in this design. Substituting inductance values into (6) yields thicknesses of each permeability. In this design, thicknesses of  $\mu_r=50$  and  $\mu_r=200$  ferrite tapes are 2mm and 1mm respectively. The whole inductor size is thus  $18\text{mm}\times 18\text{mm}\times 3\text{mm}$ . Inductances are  $0.8\mu\text{H}$  at  $0\text{A}$  and  $0.3\mu\text{H}$  at  $10\text{A}$ . DCR is thus  $5.7\text{m}\Omega$ .

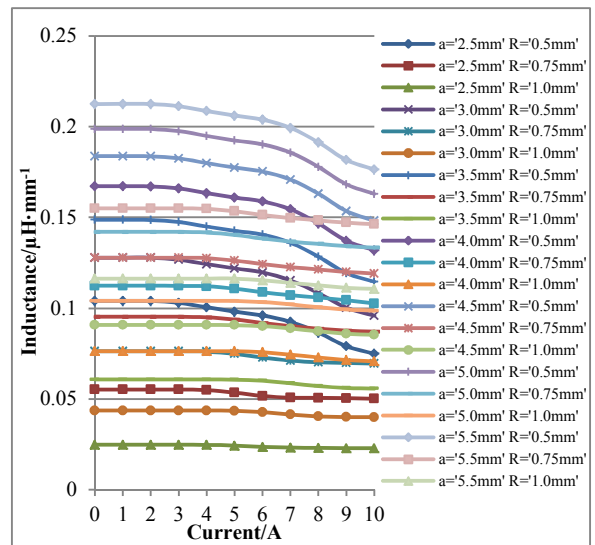


Fig. 8 Inductance versus current for  $\mu_r=50$  ferrite tapes.

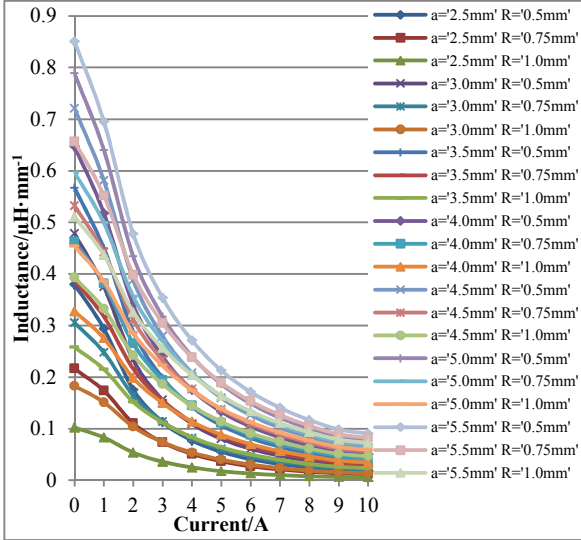


Fig. 9 Inductance versus current for  $\mu_r=200$  ferrite tapes.

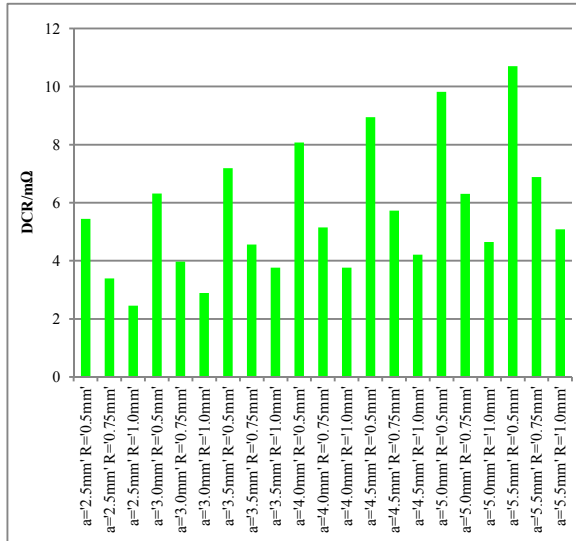


Fig. 10 DCR of the sixteen-hole two-permeability nonlinear inductor.

#### IV. PROTOTYPE AND EXPERIMENT

A 18mm×18mm sixteen-hole two-permeability LTCC nonlinear inductor prototype is made in this section to verify the proposed model. The prototype picture and the structure of the inductor are shown in Fig. 11. The integrated magnetic core is composed of 1mm thickness 40010 ferrite tapes whose relative permeability is 50 and 2mm thickness 40011 ferrite tapes whose relative permeability is 200. The inductance versus current curve of the prototype is obtained by measuring the current ripple amplitude and the off time in a 5V input, 1.2V output DC/DC converter. The result is illustrated in Fig. 12. The results obtained from the model and complete simulation are also illustrated in Fig. 12 for comparison. It can be observed that the proposed model correlates very well with

the simulation. However, some differences exist between the model, simulation and the prototype test results. There are two reasons for this error. Firstly, the prototype is made manually, the position of the holes are not precisely drilled on the substrate as in the simulation and modeling. Secondly, the BH curve of the prototype may be non-ideal, which introduces some inconsistency between the modeling and simulation.

A chip inductor is selected to do an efficiency comparison. Parameters of both the chip inductor and the nonlinear inductor are listed in Table I. Both inductors are applied in a 750kHz switching frequency, 5V input, 3.6V output DC/DC converter to test the efficiency. Fig. 13 shows the efficiency curves. It is demonstrated that the nonlinear inductor can help improve the efficiency especially at light load.

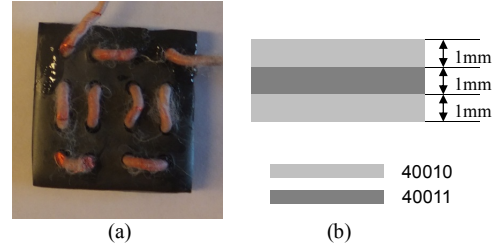


Fig. 11 Sixteen-hole two-permeability. (a) Picture of the prototype. (b) The cross-section area.

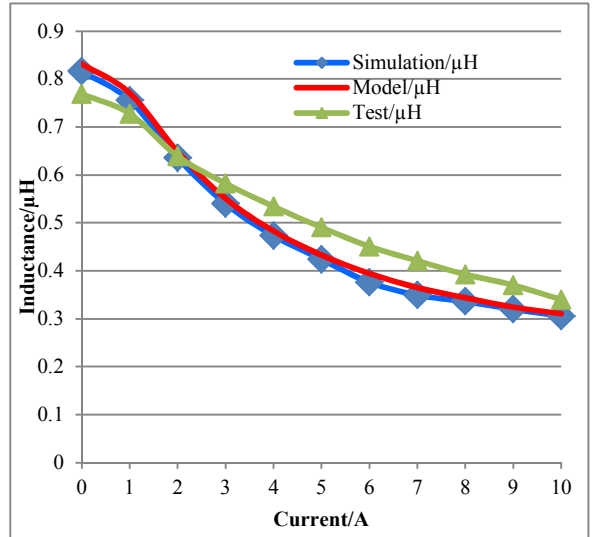


Fig. 12 The inductance curves based on model, simulation, and test.

TABLE I PARAMETERS OF THE TWO INDUCTORS

Items	DCR (mΩ)	Inductance (μH)
Chip inductor	7.5	0.3
Nonlinear inductor	7.4	0.34~0.77

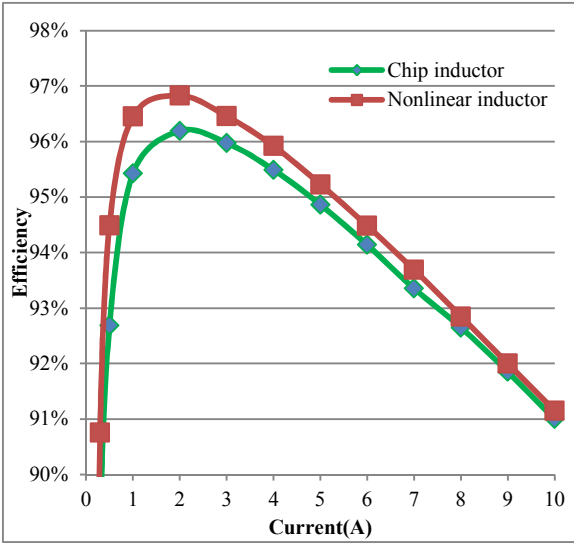


Fig. 13 The efficiency curve of the converter with different inductors.

## V. CONCLUSION

This paper focuses on the design of a rectangle shape multi-hole multi-permeability nonlinear inductor. A new model for inductance calculation is proposed. The proposed model can significantly simplify the complicated electromagnetic analysis of the nonlinear inductors by breaking down the inductor into three basic units. The calculation results of the proposed model highly agree with the simulation results and the prototype test results. As the experimental test shows, by using a nonlinear inductor in a DC/DC converter, the efficiency can be improved at light load.

## REFERENCES

- [1] Dallago, E.; Passoni, M.; Venchi, G., "Analysis of High-Frequency IGBT Soft Switching Buck Converter With Saturable Inductors," *Power Electronics, IEEE Transactions on*, vol.22, no.2, pp.407,416, March 2007.
- [2] Shu Fan Lim; Khambadkone, A.M., "Non linear inductor design for improving light load efficiency of boost PFC," *Energy Conversion Congress and Exposition, 2009. ECCE 2009. IEEE*, vol., no., pp.1339,1346, 20-24 Sept. 2009.
- [3] Harada, K.; Sakamoto, H.; Harada, K., "Saturable inductor commutation for zero voltage switching in DC-DC converter," *Magnetics, IEEE Transactions on*, vol.26, no.5, pp.2259,2261, Sep 1990.
- [4] Saito, R.; Ushiki, S., "Reduced-resonant-current zero-voltage-switched forward converter with unsaturated-region resonance of saturable inductor," *Telecommunications Energy Conference, 1991. INTELEC '91, 13th International*, vol., no., pp.151,158, 5-8 Nov 1991.
- [5] Ferreira, J.A.; Van Ross, A.; Van Wyk, J.D., "A generic soft switching converter topology with a parallel nonlinear network for high-power application," *Power Electronics, IEEE Transactions on*, vol.7, no.2, pp.324,331, Apr 1992.
- [6] Stadler, M.; Pforr, J., "Feed-forward control of non-linear inductors providing soft-switching of DC-DC-converters," *Power Electronics and Applications, 2007 European Conference on*, vol., no., pp.1,10, 2-5 Sept. 2007.
- [7] Stadler, M.; Pforr, J., "Zero-Voltage Switched Multi-Phase Converter utilizing nonlinear and coupled Inductors," *Applied Power Electronics Conference, APEC 2007 - Twenty Second Annual IEEE*, vol., no., pp.1038,1042, Feb. 25 2007-March 1 2007.
- [8] Alonso, J. M., M. S. Perdigao. "Magnetic control of DC-DC resonant converters provides constant frequency operation." *IEEE Electronics Lett.*, vol. 46, no. 6, pp. 440-442, Mar. 2010.
- [9] Alonso, J. M., M. A. Dalla Costa. "Investigation of a New Control Strategy for Electronic Ballasts Based on Variable Inductor." *IEEE Transactions on Industrial Electronics*, vol. 55, no. 1, pp.3-10, 2008.
- [10] Lee, S.T.S.; Chung, H.S.-H.; Hui, S.Y., "Use of saturable inductor to improve the dimming characteristics of frequency-controlled dimmable electronic ballasts," *Power Electronics, IEEE Transactions on*, vol.19, no.6, pp.1653,1660, Nov. 2004.
- [11] M. Hui Fern Lim, J.D.Van Wyk, Zhenxian Liang, "Internal Geometry Variation of LTCC Inductors to Improve Light-Load Efficiency of DC-DC Converters," *IEEE Trans. Compon. Packag. Technol.*, vol.32, no.1, pp.3-11, March 2009.
- [12] Laili Wang, Yunqin Pei, Xu Yang, Zhaoan Wang "Improving Light and Intermediate Load Efficiencies of Buck Converters with Planar Nonlinear Inductors and Variable On Time Control." *IEEE Trans. Power Electron.*, vol. 27, no. 1, pp.342-353, 2012.
- [13] Zhiwei Liu; Abou-Alfotuh, A.; Wilkowski, M., "Nonlinear inductor modeling for power converter," *Applied Power Electronics Conference and Exposition (APEC), 2012 Twenty-Seventh Annual IEEE*, vol., no., pp.1868,1871, 5-9 Feb. 2012.
- [14] Salas, R.A.; Pleite, J., "Nonlinear inductance calculations of a ferrite inductor with a 2D Finite Element model," *Electromagnetics in Advanced Applications (ICEAA), 2011 International Conference on*, vol., no., pp.986,989, 12-16 Sept. 2011.
- [15] Stefopoulos, G.K.; Cokkinides, G.J.; Meliopoulos, A.P.S., "Quadratized model of nonlinear saturable-core inductor for time-domain simulation," *Power & Energy Society General Meeting, 2009. PES '09. IEEE*, vol., no., pp.1,8, 26-30 July 2009.
- [16] Deane, J. H B, "Modeling the dynamics of nonlinear inductor circuits," *Magnetics, IEEE Transactions on*, vol.30, no.5, pp.2795,2801, Sep 1994.
- [17] Stadler, A.; Gulden, C.; Stolzke, T., "Nonlinear inductors for active power factor correction circuits," *Power Electronics and Motion Control Conference (EPE/PEMC), 2012 15th International*, vol., no., pp.LS7b-2.1-1,LS7b-2.1-4, 4-6 Sept. 2012.